Geology and REE Mineralization of the Hoidas Lake–Nisikkatch Lake Area Revisited

Charles Normand, Brian McEwan [1], and K.E. Ashton

Normand, C., McEwan, B., and Ashton, K.E. (2009): Geology and REE mineralization of the Hoidas Lake–Nisikkatch Lake area revisited; *in* Summary of Investigations 2009, Volume 2, Saskatchewan Geological Survey, Sask. Ministry of Energy and Resources, Misc. Rep. 2009-4.2, Paper A-3, 17p.

Abstract

Felsic orthogneisses and migmatites are the dominant bedrock constituents in the Hoidas-Nisikkatch lakes area of the Zemlak Domain. Intermediate rocks and amphibolites, locally associated with garnet-biotite-sillimanite-graphite pelitic gneisses and diatexites, constitute less than 10% of the rocks. The first two phases of deformation are homogeneously developed throughout the map area. Although the third phase of folding is responsible for the regionally developed northeast-trending structural grain, it is heterogeneously developed. The structural grain over large areas to the northwest of the lakes is controlled by east-southeast–trending, first- and second-generation foliations, and is only mildly affected by D_3. Southeast of the lakes, between the Hoidas-Nisikkatch Fault and the Black Bay Fault, all structures are intensely transposed parallel to the third-generation foliation. The fourth phase of deformation was weak and produced open folds with north- to north-northwest–oriented steeply dipping axial planes. Upper amphibolite facies metamorphism was responsible for the formation of the garnet-biotite-sillimanite-graphite rocks during D_2. Similar levels of metamorphism characterize the garnet-bearing amphibolites, but in the latter case it is not clear if growth of garnet is associated with D_2 or D_3.

North-northeast– to east-northeast–oriented REE-mineralized veins are concentrated in three areas between Hoidas and Nisikkatch lakes, and are distributed along a 9 km-long section of the Hoidas-Nisikkatch Fault. These include the JAK zone, the Hoidas South showings, and the Nisikkatch South showings. Allanite and apatite are the main carriers of the REE in the veins. The veins are massive and essentially undeformed in the JAK zone, but are folded and sheared at Hoidas South and Nisikkatch South. Structural relationships suggest that mineralization was emplaced during the latest stages of D_3. A published preliminary monazite age of 1.87 Ga for the mineralization suggests that compressive deformation coaxial with D_3 persisted for a long period of time, potentially extending the previous estimates of the lower age limit of D_3 by about 30 Ma. Older pyroxenite and peridotite dikes, REE-mineralized veins, and younger Uranium City–type mafic dykes and lamprophyres are distributed along a ~20 km-wide corridor in orthogneiss-dominated terrains of the Zemlak Domain adjacent to the Black Bay Fault. This suggests that the structural boundary between the Zemlak and Train Lake domains is deeply rooted and has provided a favourable zone for the channelling of deeply derived fluids and magma for extended periods of time.

Keywords: *Hoidas Lake, Nisikkatch Lake, Ena Domain, granitoid rocks, amphibolite, upper amphibolite facies, multiple deformation, mineralization, rare earth elements, allanite, apatite.*

1. Introduction

This report presents the results of the first season of a multi-year mapping project intended to address the tectonometamorphic setting, history, and origin of rare earth element (REE) mineralization within the region straddling the Zemlak (new classification of Ashton, 2009; formerly the Ena Domain) and Train Lake domains between Buchanan Lake and Norwest Lake in the extreme northwest part of the province (Figure 1).

During the first year of this project, bedrock mapping was completed between Hoidas Lake and Nisikkatch Lake (Figure 2) during a four-week period. Special attention was paid to the structural relationships between the REE mineralization and the host rocks in order to provide a basis for understanding the regional distribution of the mineralized structures.

[1] Department of Geology, University of Regina, 3737 Wascana Parkway, Regina, SK S4S 0A2.

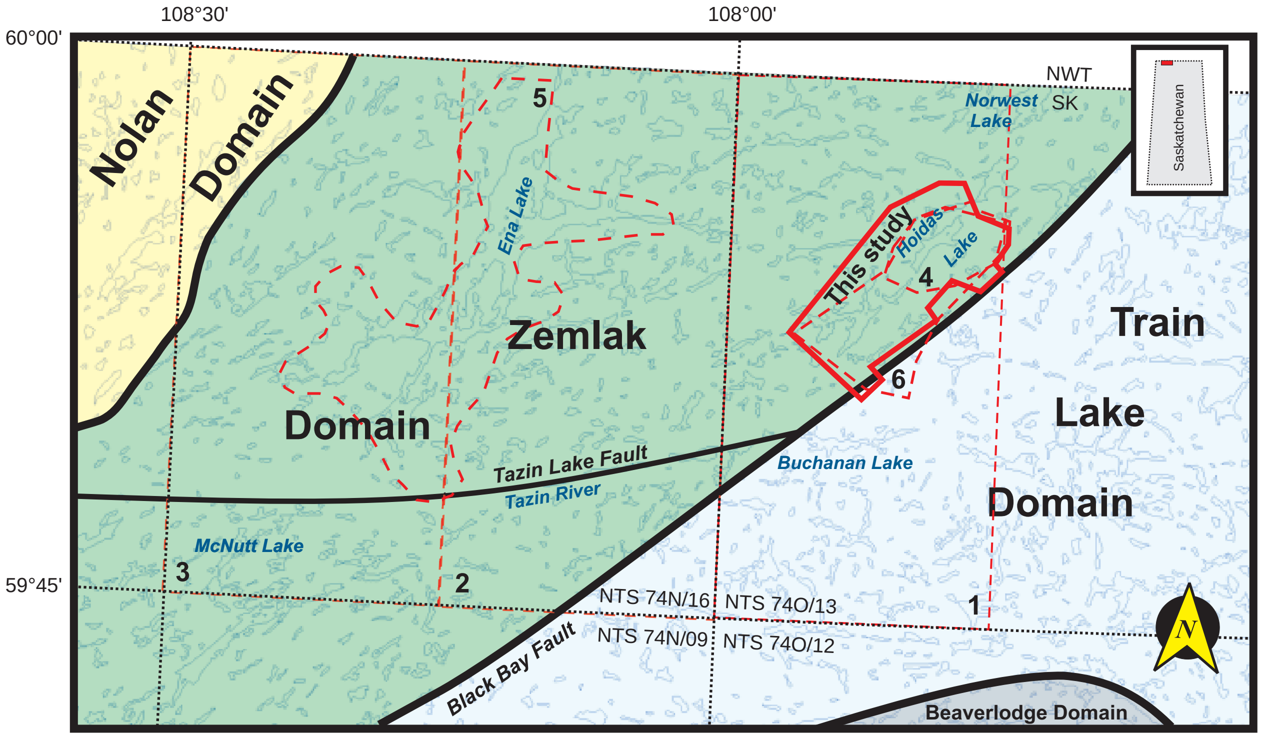

Figure 1 - Map showing the various lithotectonic domains in the area of the mapping project (solid red rectangle). Dashed red rectangles represent areas previously mapped by: 1) Koster (1965a); 2) Koster (1965b); 3) de Zoysa (1974); 4) Harvey* et al. *(2002); 5) Ashton* et al. *(2005); and 6) Gunning and Card (2005).

2. Previous Bedrock Mapping

Few studies have been published on the geology of the northernmost part of the Zemlak Domain (see Figure 1). The bedrock in the area discussed in this report was first mapped in detail by Koster (1965a) as part of his 1:63,360-scale Dardier Lake map area (west half of NTS 74O/13). Harvey *et al.* (2002) mapped the geology surrounding Hoidas Lake at the scale of 1:10 000, and gave a detailed account of REE mineralization in the JAK zone. Gunning and Card (2005) sampled bedrock, REE mineralization, and soil along three transects across the regional structural grain between Nisikkatch and Hoidas lakes, and studied the mineralized veins in the JAK zone.

3. General Geology

Rocks exposed in the area surrounding Hoidas Lake and Nisikkatch Lake form part of the Zemlak Domain, and consist principally of upper amphibolite facies augen granodiorites, tonalites, leucogranites, and lesser proportions of intermediate rocks, amphibolites, and pelitic gneisses and diatexites. The age and tectonic setting of these rocks north of the Tazin Lake Fault are poorly constrained. The crystallization age of the arc-type Ena Lake granodiorite-tonalite, which is similar to the augen granodiorites in the Hoidas Lake area, was determined at 2325 ±7 Ma (Ashton *et al.*, 2007). A secondary zircon from the same sample yielded a 1922 ±16 Ma metamorphic age (Ashton *et al.*, 2007). Altogether, up to four phases of folding have been recognized in the Ena Lake (Ashton *et al.*, 2005) and Hoidas Lake and Nisikkatch Lake (Harvey *et al.*, 2002; Gunning and Card, 2005) areas. The Taltson age (Ashton *et al.*, 2009) D_1-D_2 phases produced an east-southeast–trending composite S_1-S_2 fabric that overprints 1.97 to 1.93 Ga leucogranites. The D_3 phase is associated with tectonic activity along the Snowbird tectonic zone and produced a regional, northeast-oriented S_3 fabric. Open, north-trending F_4 folds were produced during D_4.

East of Hoidas Lake and Nisikkatch Lake, the Zemlak Domain is separated from rocks belonging to the Train Lake Domain by the Black Bay Fault. Multiple deformation events have been recognized from kinematic and strain analyses of this major regional structure, including early ductile, dextral brittle-ductile, and late normal brittle displacements (Tremblay, 1972; Ashton *et al.*, 2000; Bergeron, 2001; Bergeron *et al.*, 2002).

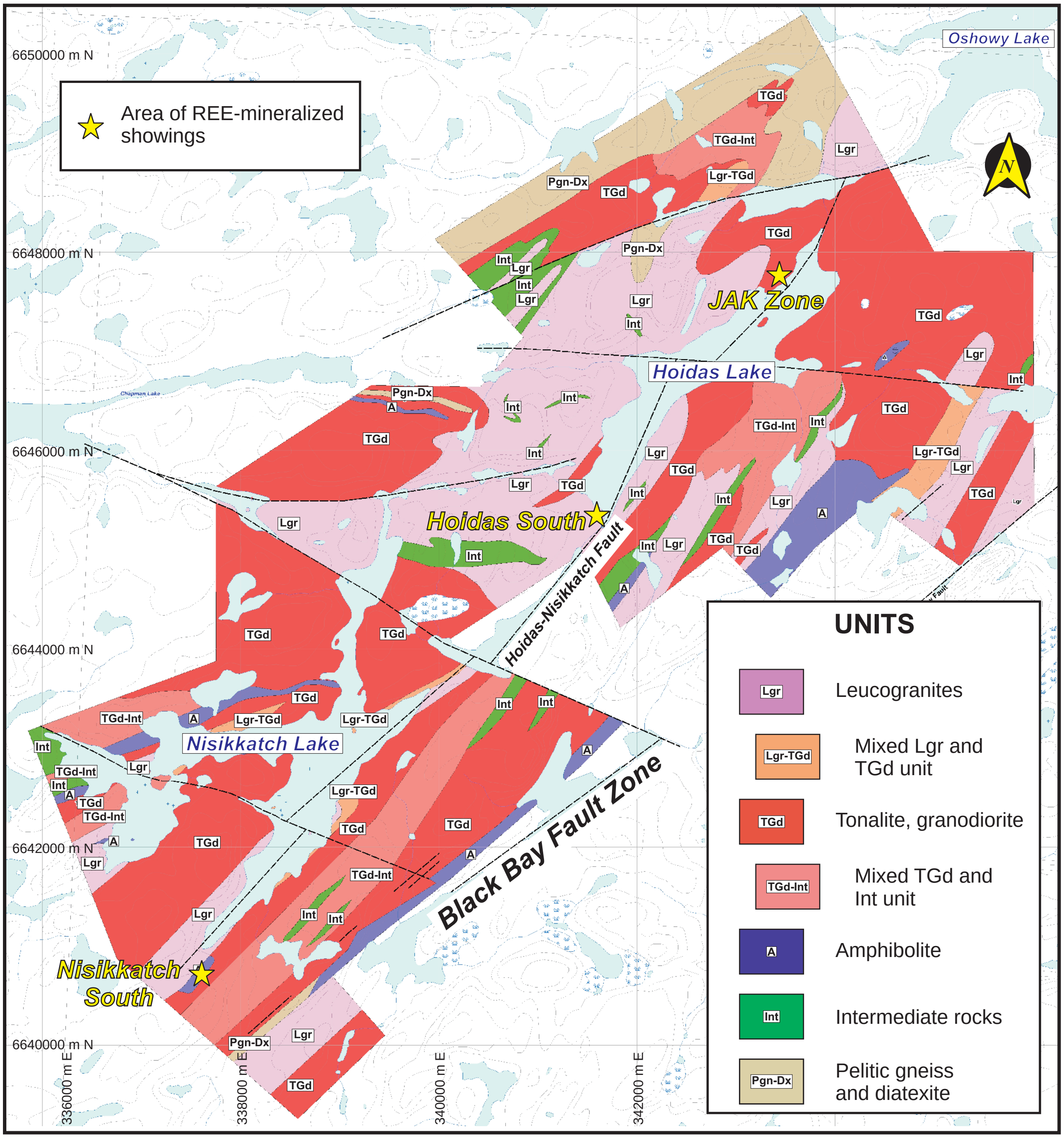

Figure 2 - Bedrock geology of the Hoidas-Nisikkatch lakes area (see the 1:20 000-scale accompanying map separate for more detail).

4. Geology of the Nisikkatch Lake–Hoidas Lake Area

Mapping in the Nisikkatch Lake–Hoidas Lake area was carried out during a four-week period in the summer of 2009 (Figure 2). Bedrock exposures are numerous and easily accessible along the shoreline of Nisikkatch Lake, but much less so at Hoidas Lake. Most of the geological data was acquired from sixteen traverses that covered 2 to 3 km-wide strips on the southeast and northwest sides of both lakes. Detailed data were collected at stations spaced 200 to 300 m apart, whereas summary notes were recorded between stations. Station locations were recorded using a Dell AXIM X51v GPS receiver. All the locations reported in this study are given in UTM coordinates using the North American Datum of 1983 (in Zone 13). High, low, and average (n=10) magnetic susceptibility measurements were collected using a Kappameter KT-9 (Exploranium) instrument. A Science Applications International

Corporation (SAIC) handheld GR-135 Plus Radioactive Isotope Identification Device (RIID) was used to locate radioactive sources and obtain estimates of K, U, and Th bulk rock concentrations.

Five distinct rock units representing greater than 70% of any particular outcrop area were mapped at the scale of 1:20 000 (see accompanying map separate). They comprise older intermediate rocks, amphibolites, tonalites and granodiorites and their gneissic equivalents, pelitic gneisses and diatexites, and younger leucogranites. The transition between these different rock types is commonly gradational, and the rocks are intensely intermixed and folded. Where intermixing of rock units is prevalent, subunits comprising a mixture of >70% of two of the distinct units have been used.

a) Unit Descriptions

Intermediate rocks (map unit Int) occur as tabular bodies less than 200 m thick that commonly display a homogeneous and massive texture at the metre scale. Locally, compositional layering at the centimetre to metre scale is observed. The rocks are composed of a fine- to medium-grained (0.5 to 1.0 mm on average) assemblage dominated by plagioclase feldspar and mafic minerals displaying a salt and pepper texture on weathered surfaces. Quartz is generally present in amounts <5% by volume. In rare samples, the proportion of quartz may exceed 10% by volume. The rocks have a colour index that varies between 15 and 35, and return low K RIID readings (1 wt. % on average). Clinopyroxene and amphibole are the most abundant mafic minerals, whereas biotite is present locally in small amounts. The average magnetic susceptibility varies between 11.7 and 127 [2] at 22 stations where the rocks are homogeneous, although the data presents a bimodal distribution centered on the values of approximately 25 and 55. A network of late, crosscutting and anastomosing, light-coloured and coarse-grained feldspar-clinopyroxene dykelets containing variable proportions of quartz is commonly present (Figure 3). The distribution of the dykelets is irregular; they never comprise more than ~5% by volume of a particular outcrop and their contact with the host rocks is sharp in most cases.

Amphibolites (map unit A) are distinguished from the intermediate rocks by their grain size (medium to coarse-grained, 1 to 2 mm on average), the presence of higher proportions of mafic minerals (colour index >35) and common compositional layering, which has been interpreted by Gunning and Card (2005) to indicate a supracrustal origin. The predominant mafic mineral is hornblende. It forms equidimensional, 1 to 2 mm grains associated with plagioclase feldspar giving weathered surfaces a salt and pepper texture. Where present, biotite is concentrated along foliation planes and is interpreted to be retrograde in origin. A green pyroxene, probably a species of the diopside-hedenbergite series, is locally the prevalent ferromagnesian mineral in the more leucocratic layers, and in light-coloured, medium- to coarse-grained dykes and irregular segregations. The dykes occur as individual bodies with sharp contacts, locally produce an agmatitic structure or, where the rock is highly strained, are transposed and shredded parallel to a third-generation foliation. Up to 40% quartz is present in the dykes, but is absent in the segregations. Average magnetic susceptibility measurements of amphibolites vary between 6 and 66, with most data concentrated around 10.

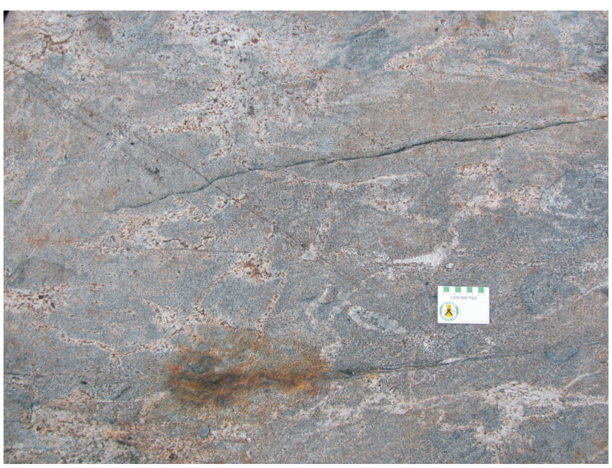

Figure 3 - Photograph showing a typical salt and pepper–textured intermediate rock cut by an anastomosing network of white clinopyroxene-feldspar dykelets (UTM 342788 m E, 6645324 m N). The scale card in this and all other pictures of this report is graduated in centimetres.

A locally garnet-rich (up to 20 vol. %) variety of amphibolite, that forms a thick (up to 500 m) 8 km-long tabular body oriented parallel to the main structural grain, is exposed east of Hoidas and Nisikkatch lakes (Figure 2). The amphibolite is compositionally layered, and comprises two types of alternating layers that measure between 1 and 30 centimetres thick. Mafic layers are composed of 50 to 90% hornblende, 10 to 50% plagioclase feldspar and, locally, garnet. Two types of leucocratic layers occur. In the first type, the minerals are the same as those present in the mafic layers, but the colour index varies between 15 and 30. The second type of leucocratic layer is characterized by the presence of a green pyroxene in place of hornblende. Although garnet was identified in outcrops of amphibolite exhibiting pyroxene-bearing leucocratic layers, its occurrence was restricted to the hornblende-rich mafic layers; it was not observed in direct contact with the pyroxene. Typical mineral assemblages consist of amphibole+plagioclase+garnet±quartz and amphibole+plagioclase+clinopyroxene±quartz. The variation in mineralogical composition of the

[2] Magnetic susceptibility in 10^{-3} SI units.

leucocratic layers is attributed to variation in chemical composition of the rocks.

Where garnet is present, it forms pink-red crystals measuring up to 3 cm in diameter that are frequently rimmed by symplectic (discernible with the naked eye) assemblages of amphibole and plagioclase feldspar (Gunning and Card, 2005). The symplectic rims are commonly framed by an external rim of amphibole crystals measuring 2 to 3 mm in diameter (Figure 4). Flattened rims around garnet crystals are observed where a third-generation foliation is strongly developed. The presence of graphite was noted in a thin, dark grey, quartz-rich lens of unknown origin at one location.

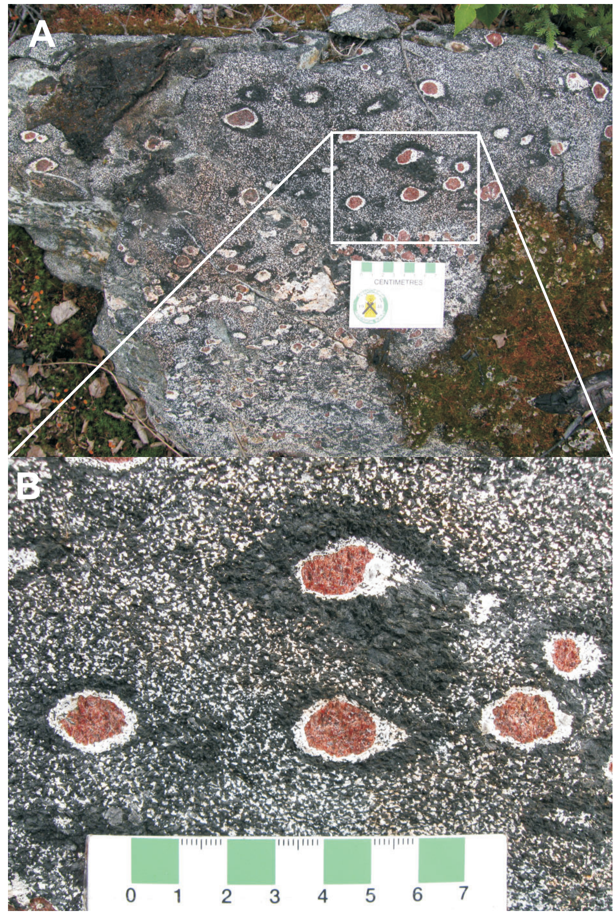

Figure 4 - A) Garnet porphyroblasts with inner decompression coronas and outer amphibole rims in amphibolite. B) Close up of garnet porphyroblasts shown in A. Note how some of the coronas appear flattened (UTM 344072 m E, 6645732 m N).

Grey to pinkish grey tonalitic to granodioritic gneisses (map unit TGd) are the oldest granitoid rocks. They vary widely in their mineralogical composition, intensity of deformation, and level of partial melting or veining. Rock types are difficult to map individually as, for example, an amphibolite or a tonalite may be intimately interlayered with granodiorite and younger pink leucogranites. For this reason quartz diorites, tonalites, quartz monzonites, granodiorites, and their gneissic equivalents, were grouped as a single unit.

All early granitoid rocks are medium to coarse grained. The best preserved granodiorites contain up to 5% pink tabular alkali feldspar phenocrysts by volume, measuring <5 cm in length. This unit corresponds to the megacrystic monzogranite of Gunning and Card (2005). Deformed types have a distinctive augen texture and may be the equivalent of the 2325 Ma Ena Lake granodiorite-tonalite described by Ashton *et al.* (2005, 2007). Average magnetic susceptibility measurements vary between 10 and 37, with most values averaging 30.

Tonalites and tonalitic gneisses, which weather grey to pinkish grey, are generally medium grained and contain 10 to 25 vol. % combined hornblende and biotite. The more leucocratic varieties display a streaky texture defined by flat, finely granular aggregates of mafic minerals oriented parallel to the main foliation in the rock. Some varieties are intimately interlayered with amphibolites and granites and display a darker grey or a pinkish colour. Typical RIID K readings oscillate around 2 wt. %. Intermixed tonalites, granodiorites, and intermediate rocks together make up greater than 70% of the bedrock over large portions of the mapped area and have been mapped separately (map unit TGd-Int).

Foliation-parallel layers, enclaves, boudins, and schlieren of both intermediate rocks and amphibolite were noted in the granodioritic, tonalitic, and granitic gneisses.

Pelitic gneiss and diatexite (map unit Pgn-Dx) are restricted in their occurrence. They are present principally in the northeast portion of the map area and on the northwest side of the southern termination of the larger layer of garnet-bearing amphibolite (Figure 2). The rocks are medium- to coarse-grained, and most commonly exhibit a mixed light grey to creamy to pink colour on outcrops. They commonly contain up to 20% garnet by volume (individual crystals measure 0.5 to 1.0 cm in diameter on average, rarely up to 5 cm), up to 5% greenish grey acicular to prismatic sillimanite (Figure 5) and rare graphite flakes. Biotite is present in major proportions in the melanosome layers of migmatized pelitic gneisses (Figure 6), but forms a minor constituent of diatexites. Salt and pepper–textured, fine- to medium-grained intermediate rocks and amphibolites (Figure 7) are intimately associated with the pelitic gneisses and diatexites. Also common are coarse-grained veins and layers of grey, quartz-rich material (up to 80% quartz; Figure 8) that occasionally show diffuse contacts with the host rock. The diatexites contain filamentous, and at times almost nebulitic, remnants of biotite-rich melanosome oriented parallel to an early, composite S_1-S_2 fabric (Figure 9). The composition and texture of the diatexites suggest that they originated from extensive partial melting of a pelitic (or psammopelitic) protolith. Near their contact with the pelitic gneisses and diatexites, the tonalites and amphibolites locally contain garnet.

Figure 5 - Pelitic/psammopelitic diatexite showing greenish grey prismatic sillimanite crystals (Sil) in garnet. Other minerals present in the diatexite include feldspar, quartz, magnetite, ilmenite, minor biotite and traces of graphite (UTM 340885 m E, 6648335 m N).

Sillimanite-garnet-biotite gneisses were reported to occur in association with amphibolites south of Ena Lake and a possible volcanic origin for the amphibolites was proposed by Ashton *et al.* (2005). Examination of Koster's (1965a, 1965b) and Ashton *et al.'s* (2005) maps indicate that the latter sillimanite-garnet-biotite gneisses may represent the southernmost extension of the unit present in the northeast part of our mapped area.

Leucogranites (map unit Lgr) include three texturally different types. With the exception of younger dykes (see below), they are the latest plutonic rock types to have been emplaced. The prevalent type is pink and contains less than 5% mafic minerals dominated by biotite and magnetite. This variety of leucogranite cuts a second type that displays a slightly deeper pink colour on weathered surfaces. The latter is also distinguished by the presence of between 5 and 8% dark minerals in which pyriboles predominate. The third type is grey-pink in colour and is characterized by the presence of ~35% 1 to 3 mm equant smoky grey alkali feldspar crystals. It is intimately associated with the pink, prevalent type of leucogranite. Average magnetic susceptibility measurements from the leucogranites vary widely (13 to 43), although the pyribole-bearing varieties present values below 20.

Intermixed leucogranites, tonalites, and granodiorites make up together greater than 70% of the bedrock over large portions of the mapped area and have been mapped separately (map unit Lgr-TGd). Stromatic migmatites that consist of uniformly alternating, centimetre-thick layers of medium-grained pink leucogranitic leucosome (60 to 65% by volume) and thinner grey to dark grey equigranular melanosome, in which biotite is the predominant mafic mineral, were assigned to this unit.

Dykes are numerous in the area and vary widely in composition. The earliest dykes consist of medium- to coarse-grained mafic (amphibolite, diorite, gabbro, pyroxenite) and felsic (quartz monzonite, granite, aplite, granite pegmatite) rocks. Irrespective of their nature, some of these dykes are strongly foliated and transposed parallel to S_1-S_2, others cut S_1-S_2 and are affected by F_3 folds, and still others show few evidences of ductile deformation (pyroxenites in particular). More interesting, however, are two late sets of dykes that cut the main regional structures and include a very fine-grained, dark-grey mafic set and a set of ferromagnesian lamprophyres. The first set forms subvertical, east-trending dykes less than 30 cm thick. They may be the equivalent of the Uranium City and Sparrow mafic dykes described in Ashton *et al.* (2005), Ashton *et al.* (2009), and Morelli *et al.* (2009). In his Dardier Lake area report, Koster (1965a) reported finding two lamprophyre dykes. Nine lamprophyre dykes containing between 2 and 10% biotite phenocrysts measuring 1 to 5 mm in length were identified as part of this study. They form centimetre- to metre-thick, steeply dipping dykes oriented northeast

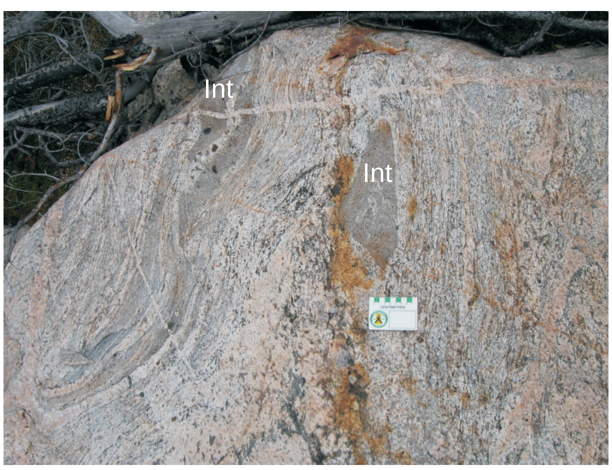

Figure 6 - Biotite-rich melanosome layers in pelitic gneiss. Note also the dark-coloured irregular inclusions of intermediate rock (Int). The larger fragment is cut by a dyke of mobilized leucosome (UTM 341981 m E, 6649090 m N).

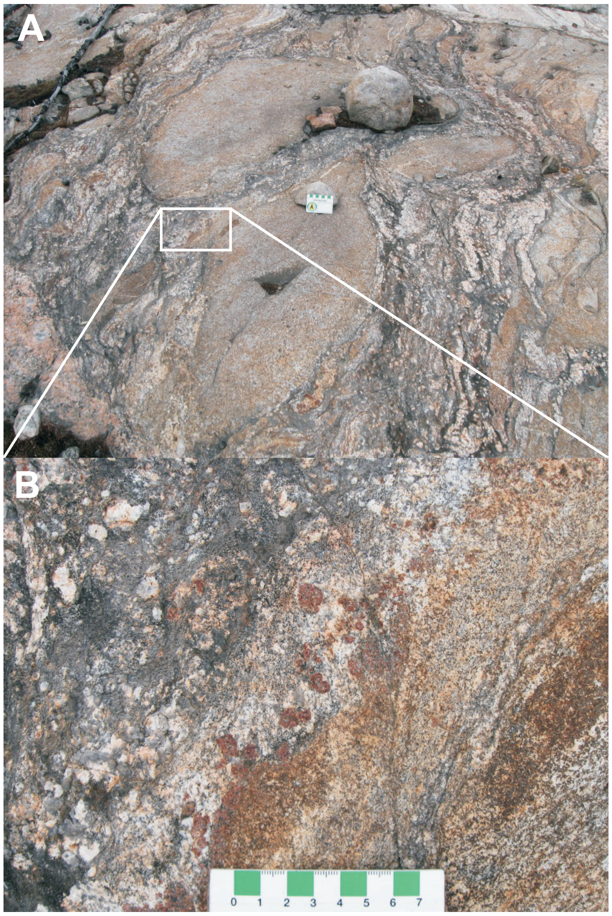

Figure 7 - A) Boudinaged amphibolite in coarse-grained, foliated, biotite-rich pelitic gneiss migmatite (UTM 341981 m E, 6649090 m N). B) Detail showing garnet-rich reaction zone between migmatite and amphibolite.

Figure 8 - Folded, grey-weathering, quartz-rich veins in rusty weathering pelitic gneiss (UTM 342100 m E, 6647894 m N).

Figure 9 - Diatexite showing garnet-rich leucosome containing filamentous remnants of biotite-rich paleosome and melanosome (UTM 341981 m E, 6649090 m N).

to east-northeast. Significantly, the occurrence of the lamprophyres is restricted to a narrow corridor, less than 300 m wide and striking 050° that extends from 475 m northeast of the JAK zone to the northwest corner of Nisikkatch Lake. This lamprophyre dyke trend corresponds roughly to that of the REE-mineralized veins. The lamprophyre dykes exhibit a brown colour (on fresh and weathered surfaces) in the northwest sector of the corridor and are green, finer grained and contain fewer phenocrysts to the southeast. This concentrated occurrence of the lamprophyre dykes contrasts with their more widespread distribution in the Beaverlodge, Train Lake, and Zemlak domains.

b) Deformation and Metamorphism

Rocks in the study area have been affected by at least four phases of plicative deformation (identified herein as D_1, D_2, D_3, and D_4). The principal structural element visible at the outcrop scale is a composite S_1-S_2, variably penetrative foliation defined by flattened or elongated single mineral grains, alternating leucosome and melanosome, and transposed primary compositional layering. The latter is locally observed in amphibolites. The S_1-S_2 foliation varies from almost imperceptible, especially in the intermediate rocks and amphibolites, to strong – the latter being best developed in the granitoids. Although the nature of S_1-S_2 depends on the lithology in which it formed, at the scale of the mapped area, its intensity is homogeneously developed.

First-generation fold (F_1) hinges associated with D_1 were not observed. Outcrop-scale second-generation folds (F_2) deforming the first-generation foliation (S_1) are uncommon; however, on the few outcrops where they were observed, the folds were tight to isoclinal (Figure 10). F_2 folds were observed in pink leucogranite injected into a

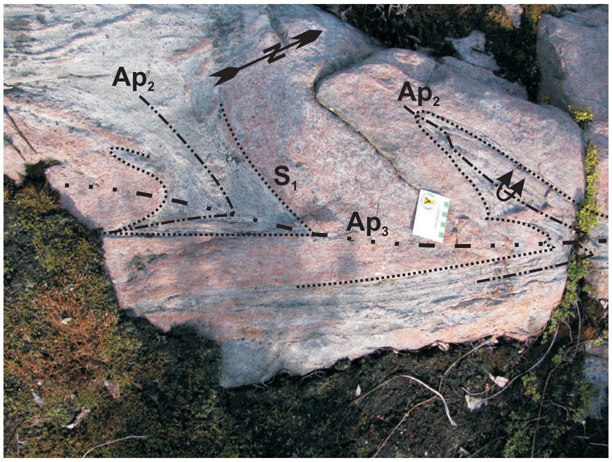

Figure 10 - Photograph showing interlayered pink leucogranite and tonalite affected by three phases of deformation (UTM 341939 m E, 6645620 m N). Interlayering of the leucogranite and tonalite is parallel to the S_1 foliation, which has been isoclinally folded (Ap_2) during D_2. The second-generation folds have been refolded by F_3. Dash-double dot lines denote axial traces of F_2 folds; double dash-triple dot line denotes axial trace of F_3.

tonalitic gneiss, implying a long, protracted history of crustal melting, possibly starting as early as D_1 and extending into the latest stages of D_2.

A third-generation foliation (S_3) associated with D_3 overprints all rocks. Whereas the composite S_1-S_2 foliation is uniformly developed throughout the study area, the intensity of S_3 is highly variable. As a general rule, the rocks show increasing levels of D_3-associated strain going from northwest to southeast towards the Black Bay Fault (see also Harvey *et al.,* 2002 and Gunning and Card, 2005). On the northwest sides of Hoidas and Nisikkatch lakes, large areas are more or less weakly affected by D_3 and possess a predominant S_1-S_2 fabric oriented east-southeast. In contrast, on the southeast side of Hoidas and Nisikkatch lakes, it is common to encounter only one direction of foliation where all rock types and S_1-S_2 have been transposed parallel to S_3, which defines a regional northeast-trending structural grain. Exposures of various types of granitoid rocks that display S_3-parallel ultramylonitic fabrics over thicknesses exceeding 10 m are common within 500 m of the Black Bay fault. Rotated alkali feldspar sigma and, less commonly, delta porphyroclasts indicate a dextral component of shear, consistent with the displacement along rare shear bands.

As indicated above, strain levels associated with D_3 vary widely. As a result, F_3 folds vary from open to isoclinal. They are open to the northwest of Hoidas and Nisikkatch lakes and become tight to isoclinal with steeply dipping northeast-trending axial planes towards the Black Bay Fault (Figures 10 and 11). S_3 is axial planar to the F_3 folds. F_3 fold axes and axis-parallel stretching lineations form two populations that plunge gently to moderately to the northeast and southwest. The easternmost expression of the Black Bay

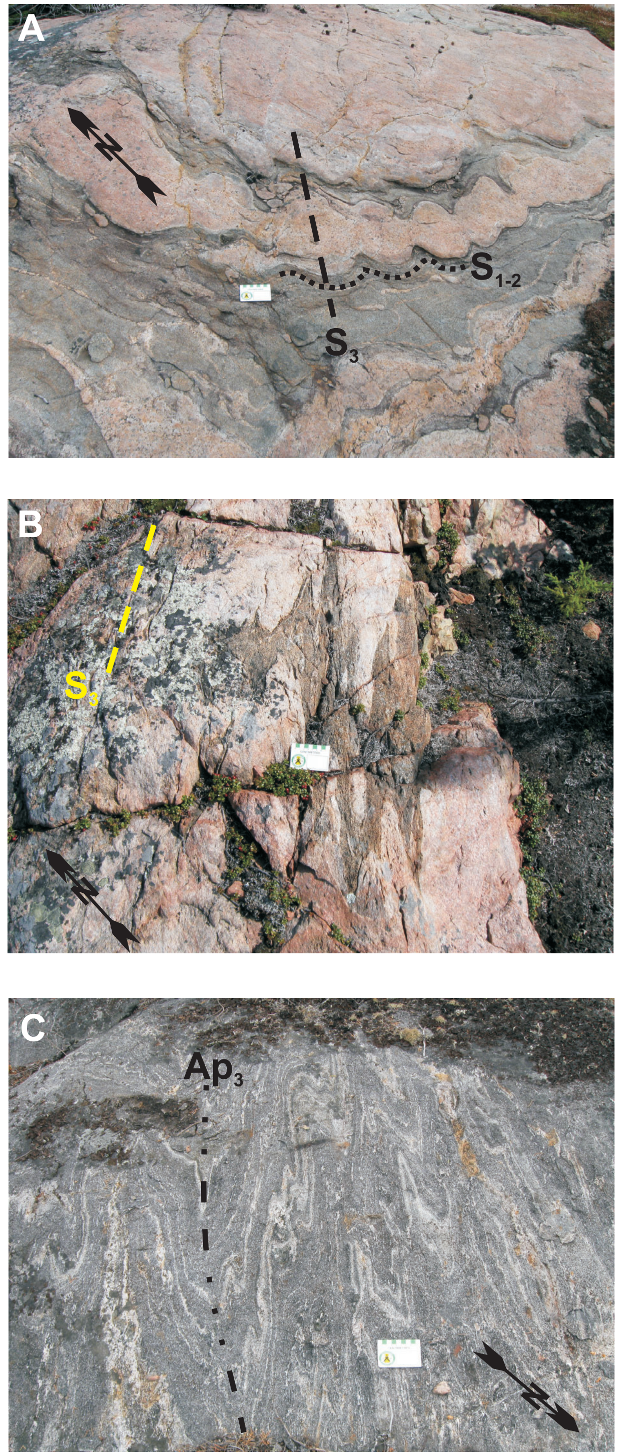

Figure 11 - Series of photographs showing variable D_3-associated strain exemplified by: A) open F_3 folding in interlayered pink leucogranite and amphibolite northwest of Hoidas Lake (UTM 341768 m E, 6647364 m N); B) tight F_3 folds in interlayered pink leucogranite and amphibolite southeast of Hoidas Lake (UTM 344850 m E, 6646950 m N); and C) tight F_3 folds in layered amphibolite near the Black Bay Fault southeast of Nisikkatch Lake (UTM 339116 m E, 6640957 m N).

Shear/Fault zone is a late, post metamorphic, lineament that follows the Tazin River and cuts the main S_3 fabric clockwise by ~10° (see Figure 2).

Only gently undulating fourth-generation folds (F_4) with steeply dipping north-northwest–trending axial planes were imparted to the rocks as a result of D_4.

The comparatively coarse-grained and recrystallized nature of the rocks, locally extensive partial melting, and mineral assemblages identified in the field collectively indicate that upper amphibolite facies metamorphic conditions were attained in the area of Nisikkatch and Hoidas lakes, although orthopyroxene (indicative of granulite facies) was reported by Koster (1965a) and Harvey *et al.* (2002) to occur in felsic orthogneisses and amphibolites. In general, the rocks lack diagnostic low-variance mineral assemblages that enable estimation of the pressure (P) and temperature (T) conditions responsible for their metamorphism. However, the assemblage biotite+plagioclase feldspar+sillimanite+quartz+K-feldspar+garnet (without muscovite, cordierite or orthopyroxene) can be used to make a first-order approximation of the P and T conditions during formation of the pelitic gneisses and diatexites. The P-T range is constrained by reactions 1 (Thompson, 1982), 2, and 3 (Winter, 2001) below:

Biotite + Sillimanite + Plagioclase + Quartz = Garnet + K-feldspar + liquid (1)

Muscovite + Quartz + liquid = Sillimanite + K-feldspar + vapour (2)

Biotite + Sillimanite = Garnet + Cordierite + K-feldspar + liquid (3)

and suggests pressures of between 4.5 and 7.5 kbar, and temperatures in the 710° to 770°C range. The sharp intrusive contacts of the diatexites and general absence of nebulites suggest that partial melting of the pelitic protolith from which they were derived took place under stress. The timing of formation of the above mineral assemblage is constrained by the sequence of deformation events exhibited by the rocks. On the northwest side of Hoidas Lake, pelitic gneisses and diatexites locally exhibit an east-southeast trend of the S_1-S_2 foliation and garnet-biotite-sillimanite-graphite–bearing assemblages. Metamorphic conditions during their formation are thus coeval with D_2 at the latest.

An F_2 antiform with a shallow west-northwest–plunging axis is exposed over a width of 25 m near the northeast termination of the large amphibolite layer located southeast of Hoidas Lake (Figure 2). The amphibolite at this location is rich in garnet crystals showing amphibole+plagioclase feldspar decomposition rims (interpreted as decompression coronas by Harvey *et al.*, 2002 and Gunning and Card, 2005). The garnet crystals and their rims are locally flattened within the plane of the S_3 foliation (Figures 4 and 12). This indicates that metamorphic garnet growth occurred during or before D_3. The timing of uplift, decompression, and development of the garnet replacement-coronas are unclear, however. The coronas may have formed at any time between stress relaxation immediately following D_2, and D_3.

A regionally developed sequence of events is emerging by comparing the four phases of deformation identified in this study with those recognized by Ashton *et al.* (2005) 20 km to the west in the area of Ena Lake and those in the Uranium City area summarized in Ashton *et al.* (2009). In a recent publication addressing the significance of the deformation events in the area of Uranium City within the regional tectonic context of the southern Rae Province, Ashton *et al.* (2009) suggested the following salient points:

1) Crustal thickening during D_1-D_2 and associated partial melting was accompanied by widespread emplacement of leucogranites at 1.94 to 1.92 Ga.
2) The last major, high-grade metamorphic event in the Uranium City area took place during D_3-induced northwest-southeast shortening at 1.911 to 1.903 Ga and affected rocks on both sides of the Black Bay Fault.
3) D_4 imparted weak deformation at about 1.83 to 1.82 Ga, as a result of east-west shortening that accompanied accretion of the Nahanni–Fort Simpson Terrane to the west and final collision in

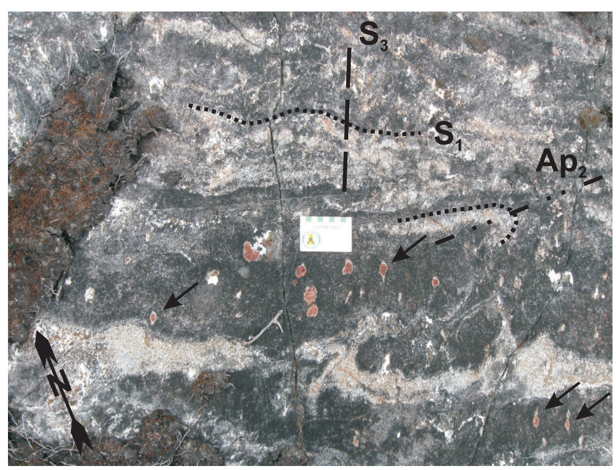

Figure 12 - Flattened garnet porphyroblasts and decompression coronas (arrows) in layered amphibolite (UTM 344156 m E, 6645745 m N). Layering is parallel to east-southeast–striking S_1 (dotted lines) and is deformed by tight F_2 folds (dash-double dot line, Ap_2, denote axial trace of F_2 fold). The porphyroblasts and rims are flattened in the plane of S_3 (dashed line) which is oriented at a high angle to the layering.

the Trans-Hudson Orogen to the east. The locally folded Uranium City mafic dykes were emplaced during this period.

The sequence of structures developed in the Hoidas and Nisikkatch lakes area correlate well with the regional scheme described above. Similarly, four phases of deformation have been identified where: 1) D_1 and D_2 are represented by a composite S_1-S_2 foliation, oriented west-northwest in large portions of the map area, and by F_2 folds that affect leucogranites; 2) a heterogeneously-developed, northeast-trending S_3 regional foliation was developed during D_3; and 3) east-west shortening during D_4 produced gently undulating F_4 folds.

In the Hoidas and Nisikkatch lakes area, deformation along the Black Bay Fault appears to have been initiated at the boundary between the Zemlak and Train Lake domains during D_3. At that time, displacements were accommodated along a number of ductile northeast-trending, S_3-parallel shear zones distributed across a wide sector that covers the distance between the Hoidas and Nisikkatch lakes. The narrow lineament defined by the Tazin River between the Saskatchewan/Northwest Territories border and Buchanan Lake (Figure 1) is, as indicated above, oriented at a ~10° angle to the regional S_3 fabric. This indicates that the lineament mirrors only the effects of late deformation along the Black Bay Fault. It is not known, however, to what phase of deformation this lineament can be attributed to. In the Uranium City area, D_4-associated movement has been described by Ashton *et al.* (2009).

5. REE Mineralization

a) Generalities

Apart from a few prospect pits opened up on quartz veins that contain traces of copper, the only other showings that have been recognized in the study area are the allanite-rich REE occurrences discovered in 1950 by Jack Lane, who was prospecting for uranium. Hogarth (1957) examined these occurrences shortly after their discovery and provided the first description of the mineral paragenesis. The REE mineralization received only sporadic attention until 1996 when Daren Resources Ltd. staked the JAK zone. Great Western Gold Corp. optioned the property from Daren Resources Ltd. in 1999 following encouraging metallurgical tests of the REE ore. The JAK zone and other known REE-mineralized showings have since been developed by Great Western Gold Corp., later renamed Great Western Minerals Group Ltd. (GWMG).

The principal mineralized zone, traced over a strike length of approximately 750 m, is located on the northwest shore of Hoidas Lake and is known as the JAK Zone (Figure 2). Extensive drilling was completed on this zone between 2001 and 2008 by GWMG. Barr Engineering Company's commissioned NI 43-101–compliant resource estimate, released by GWMG on November 20, 2009, established combined Measured and Indicated Reserves of 2 560 835 t at 2.431% total rare earth oxides at a 1.5% cut-off grade for the JAK Zone (WARDROP, 2006).

The REE-mineralized occurrences are concentrated along the Hoidas-Nisikkatch Fault (Harvey *et al.*, 2002), which is located at the transition between a relatively low-strain region west of Hoidas and Nisikkatch lakes, and a high-strain zone characterized by discrete mylonite zones that extend eastward to the Black Bay Fault (Figure 2). The REE veins are hosted by granitoid rocks at the Hoidas Lake showings, and by amphibolite at Nisikkatch South. There is little evidence of ductile deformation overprinting the veins in the JAK zone. Folding and shearing, however, has affected the veins at the Hoidas South and Nisikkatch South showings.

b) Character of the REE Mineralization

The REE mineralization is hosted by veins [3] that cut granitic to tonalitic gneisses and amphibolites of the Zemlak Domain. They were interpreted to have been the result of metasomatism-metamorphism of a pyroxene-rich ultramafic to lamprophyric vein-dyke system by Harvey *et al.* (2002). However, the lamprophyre dykes in the area are believed to be younger than the mineralization and Gunning and Card (2005) suggested that the latter have a separate alkaline igneous affinity. Individual mineralized veins have been traced on surface over 425 m in strike length, are up to 15 m in thickness, and have been multiply reactivated (WARDROP, 2006; Halpin *et al.*, 2008). They are zoned and comprise apatite-rich sections in the core, and sections that are essentially composed of silicates, including allanite, Ba-rich alkali feldspar and Ca-rich clinopyroxene, at the margins. Four generations of apatite have been recognized, which are commonly brecciated (Halpin *et al.*, 2008). Veins showing sections composed essentially of calcite, barite, quartz, and apatite were reported by Hogarth (1957), but efforts to locate this particular type by GWMG personnel were unsuccessful (J. Pearson, pers. comm., 2009). The carbonate-rich portion of the veins was interpreted to be hydrothermal in origin by Hogarth (1957). In Woolley and Kjarsgaard (2008), the deposit is included in the carbohydrothermal type.

[3] Although a portion of the mineralization is believed to have been emplaced as a silicate-rich liquid (Hogarth, 1957; Gunning and Card, 2005), the host structures show complex zoning patterns or are monomineralic and are better described as "veins".

c) Structural Context of the REE Mineralization

No previously unreported allanite-apatite–rich veins were found during mapping. A thorium anomaly (RIID reading of 474 ppm) was discovered, however, associated with a thin clinopyroxene vein cutting a ~50 m-thick, medium-grained amphibolite layer 1.4 km southeast of the JAK zone (UTM 344606 m E, 6647005 m N). Our observations of ten trenched REE-mineralized showings, in the area encompassed by the JAK zone and the southern end of Nisikkatch Lake (Figure 2; accompanying map separate), are presented below.

JAK zone: Two trenches were studied in detail in the JAK zone [Saskatchewan Mineral Deposits Index (SMDI) #1612]. In trench JK-1 (GWMG's bulk sample pit area; see Sask. Ministry of Energy and Resources assessment file 74O13-NW-0022), the mineralization is hosted by a brecciated vein measuring over 2 m wide that strikes 065° and is dipping steeply to the southeast. The vein cuts tonalite in the footwall, which contains a strongly developed subvertical north-south S_1-S_2 foliation, and pinches towards the east where it abuts a zone of medium-grained red-stained leucogranite that displays a strong S_3 mylonitic fabric oriented 044°/80°. The breccia is characterized by abundant angular fragments of highly variable size and shape that consist chiefly of clinopyroxene, allanite, and wall rock set in a matrix of apatite (Figure 13). Grain size in the apatite-rich matrix varies from coarse to very fine. In addition to extreme grain-size variation, flow structures are evident in the apatite matrix. This breccia has been interpreted as a diatreme by Pearson (2005, 2006).

Two veins cutting mixed tonalite and leucogranite were examined in the area of trench JK-2 (GWMG trench 8). The thicker vein measures 1 m from wall to wall in its widest part and is oriented sub parallel to S_1-S_2 (~019°/89°). The vein consists mostly of dark-coloured amphibole, K-feldspar, allanite and clinopyroxene, with minor proportions of hyalophane (Ba-rich alkali-feldspar) and apatite, and traces of zircon (?). The second vein measures 30 cm in thickness and is oriented 041°/69°. Early green clinopyroxene and later allanite fill the margins of the vein, whereas the core is occupied by an irregularly shaped apatite lens. The contacts of the two veins with the host rocks are sharp and they appear to be essentially unaffected by ductile deformation.

Hoidas South: A ~10 m x 25 m stripped area at the southern end of Hoidas Lake (SMDI #1611) exposes deformed REE-mineralized veins hosted by pink leucogranite that display a strongly developed S_3 fabric (Figure 14). Amphibolite layers and later clinopyroxene-apatite-allanite-hyalophane-biotite veins in the leucogranite are isoclinally folded (Figures 14C to 14E), with axial planar surfaces that parallel the regional S_3 fabric. The larger mineralized vein and immediately enveloping foliated leucogranite are folded, with a shallow southwest-plunging axis. This suggests that the veins were emplaced and deformed over an extended period of time during D_3.

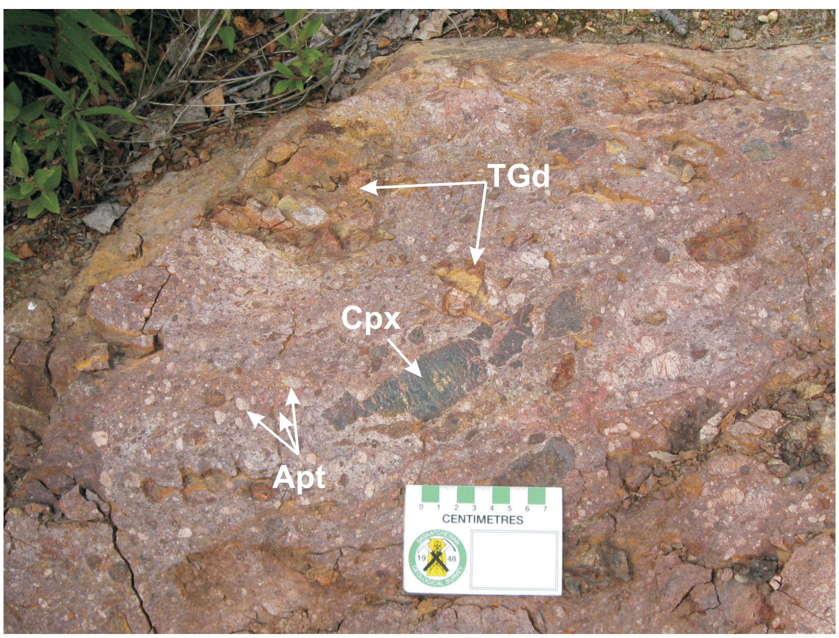

Figure 13 - Photograph of a brecciated vein in the JAK zone (trench JK-1; UTM 343419 m E, 6647737 m N). Note the strongly altered wall rock fragments (TGd), fractured clinopyroxene (Cpx) and apatite (Apt) showing extreme grain-size variation (coarse apatite fragments weather to a light colour; very fine-grained matrix apatite is red).

Wall rock alteration is difficult to recognize in the JAK zone and at Hoidas South. K-feldspar alteration is described in numerous GWMG diamond drill hole logs from the JAK zone, however, and Ba concentrations exceeding 2000 ppm are reported from all wall rock analyzed within 1 m of mineralization.

Nisikkatch South: Allanite-rich mineralization is exposed in seven small trenches near the southern end of the southern arm of Nisikkatch Lake (Figure 2), and within about 150 m of the Hoidas-Nisikkatch Fault. The trenches are distributed in a medium- to coarse-grained amphibolite layer, measuring 20 m wide and at least 350 m long and oriented ~ 035° (Figure 15). REE mineralization occurs in planar or irregular, centimetre- to metre-wide, *en echelon*, east-northeast–striking, medium- to very coarse-grained veins. The *en echelon* veins form a trend

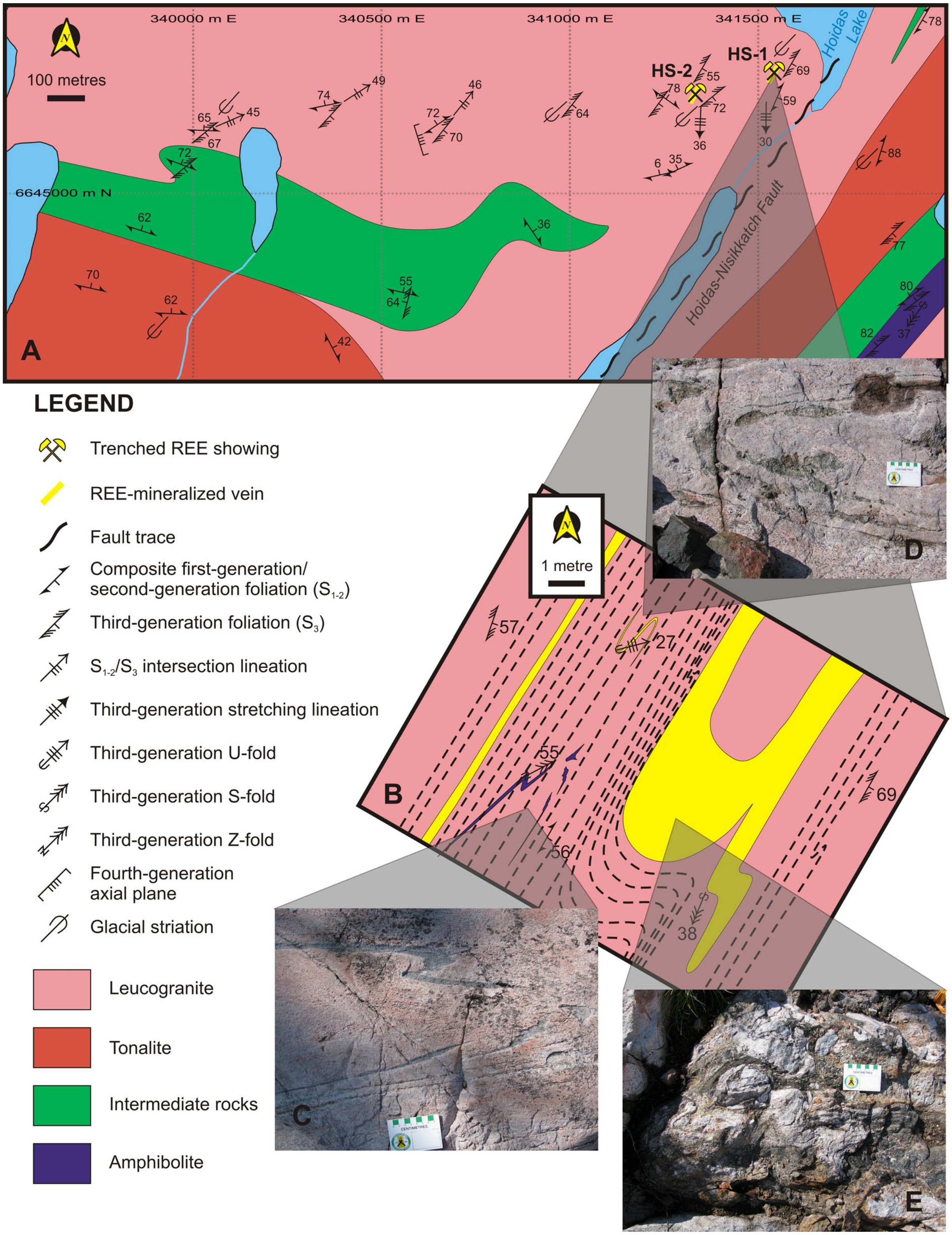

Figure 14 - A) Geological map of the southern portion of Hoidas Lake showing the location of the Hoidas South REE occurrences. B) Geological sketch of the main Hoidas South REE occurrence (UTM 341544 m E, 6645321 m N). It has been drawn at an approximate scale. C) Photograph showing an isoclinally folded amphibolite layer in strongly foliated pink leucogranite. Parasitic fold axes plunge moderately to the northeast. D) Isoclinally folded diopside-rich REE mineralized vein with axial planar surfaces parallel to the foliation in the leucogranite. E) Highly contorted clinopyroxene-hyalophane-apatite-allanite-biotite in the hinge of an isoclinally folded vein.

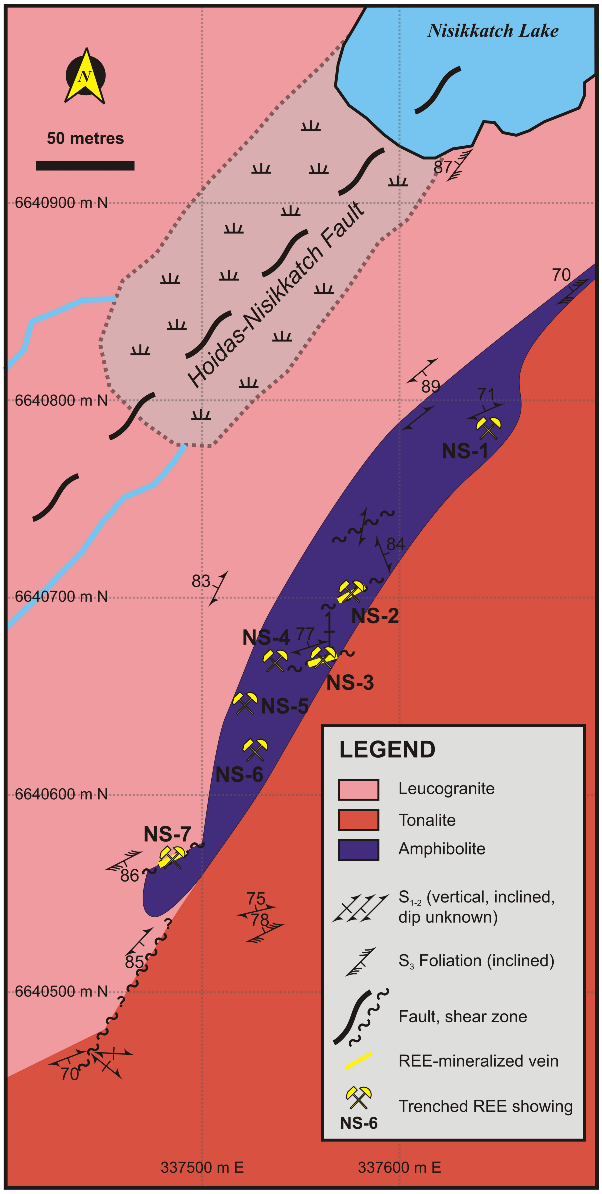

Figure 15 - Geological map showing the location of the Nisikkatch South showings in an amphibolite lens.

that parallels the strike of the amphibolite layer. Allanite-clinopyroxene–rich mineralization occupies the cores of the veins, which measure up to 1 m thick and where individual allanite crystals measuring 10 to 20 cm were observed. The allanite-clinopyroxene mineralization is included in a white feldspar matrix that contains variable, but generally low, proportions of quartz. The feldspar-rich portions are clearly "vein" material where they cut foliation in the amphibolite at a high angle. The vein contacts are diffuse where they parallel the foliation, however, suggesting replacement of wall rock (Figures 16A and 16B). Metasomatic replacement of the host amphibolite is especially well developed in trench NS-2 (Figure 15) where a mineralized vein stockwork envelops fragments of the wall rock (Figure 16C). White alkali feldspar and quartz pegmatitic dykes are spatially associated but do not contain REE mineralization.

Subvertical, east-northeast–oriented shear zones parallel and deform the veins (Figure 16D), and dissect the amphibolite. Clockwise drag of the foliation in the amphibolite at the margin of the shear zones suggests dextral, strike-slip displacement. Other evidence of deformation of the mineralization is present in trench NS-3, where the veins and foliated host rocks are gently folded (Figure 16E).

With the exception of the locally developed shear foliation, only one penetrative foliation (S_1-S_2) was observed in the amphibolites. The orientation of the latter foliation varies from northwest to northeast within a few metres, indicating that the unit was refolded during D_3. The east-northeast–striking shear zones form a ~30° clockwise angle with the northeast-striking S_3 foliation measured in the vicinity of the trenches, suggesting that the shear zones formed during D_3, likely as asymmetric extensional shear bands.

In summary, our observations of the REE-mineralized veins show that: 1) they are oriented northeast to east-northeast; 2) they crosscut the foliated host rocks and are unaffected by D_1-D_2; and 3) have been variably affected by the heterogeneously developed D_3-associated structures.

6. Discussion

The spatial association and orientation of mafic dykes, lamprophyres, and REE mineralization along a narrow belt in the Hoidas-Nisikkatch lakes area is striking. When superimposed on a map (Figure 17), the older mafic dykes and the younger diabase and lamprophyre dykes [from this study and Koster's (1965a, 1965b) map], and the REE mineralization define superimposed and parallel trends roughly paralleling the Black Bay Fault on its western side. Although the mafic dykes and lamprophyres may not be genetically and temporally related to the REE mineralization, their occurrence suggests that the structural boundary between the Zemlak and Train Lake domains is deeply rooted and has provided a favourable zone for the channelling of deeply derived fluids and magma for extended periods of time. With the above in perspective, it is interesting to note the report by de Zoysa (1974) of an 8 inch x 2 inch, foliation-parallel allanite vein in pink amphibole gneiss north of McNutt Lake and south of the Tazin Lake Fault, approximately 35 km southwest of Hoidas Lake. Although not indicated on his map, Koster (1965a) also reported the occurrence of allanite showings extending up to Norwest Lake, 8 km northeast of Hoidas Lake.

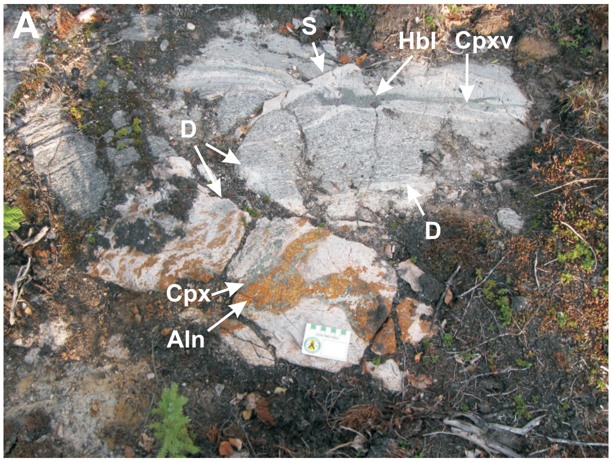

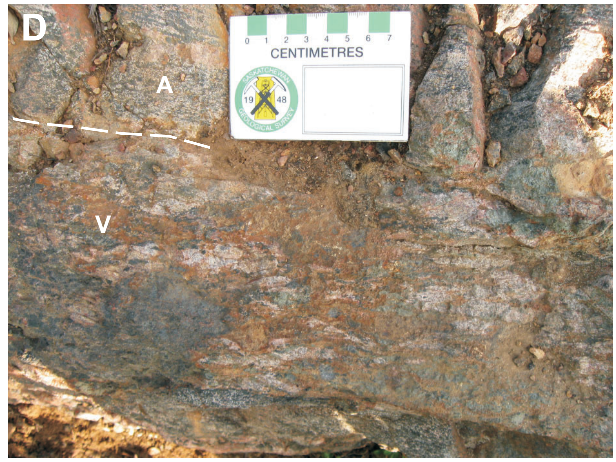

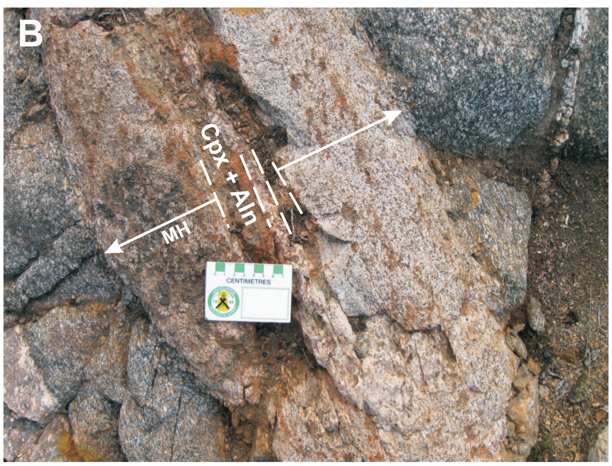

Figure 16 - A series of photographs showing various features of the REE mineralization at Nisikkatch South. A) Complex allanite (Aln)-clinopyroxene (Cpx)–bearing vein cutting amphibolite in trench NS-6. A thin splay that cuts S_1-S_2 in the host amphibolite at a high angle shows sharp contacts (S). The contacts of the vein with the wall rock are diffuse (D) where it is parallel to S_1-S_2, due to metasomatic replacement. A clinopyroxene vein (Cpxv) that cuts a hornblende (Hbl) vein can be seen in the upper right end of the photograph (UTM 337526 m E, 6640623 m N). B) Thin allanite-clinopyroxene vein with thick, symmetrically-developed metasomatic replacement halo (MH) of wall rock amphibolite in trench NS-3 (UTM 337561 m E, 6640669 m N). C) Photograph showing wall rock (A) replacement (MH) at the margins of vein material (VM) in trench NS-2 (UTM 337576 m E, 6640703 m N). D) Sheared vein (V) in amphibolite (A) in trench NS-7 (UTM 337485 m E, 6640572 m N). The shear foliation is oriented 060°/86°. E) Folded S_1-S_2–parallel allanite-clinopyroxene vein (V) in amphibolite in trench NS-3 (UTM 337561 m E, 6640669 m N).

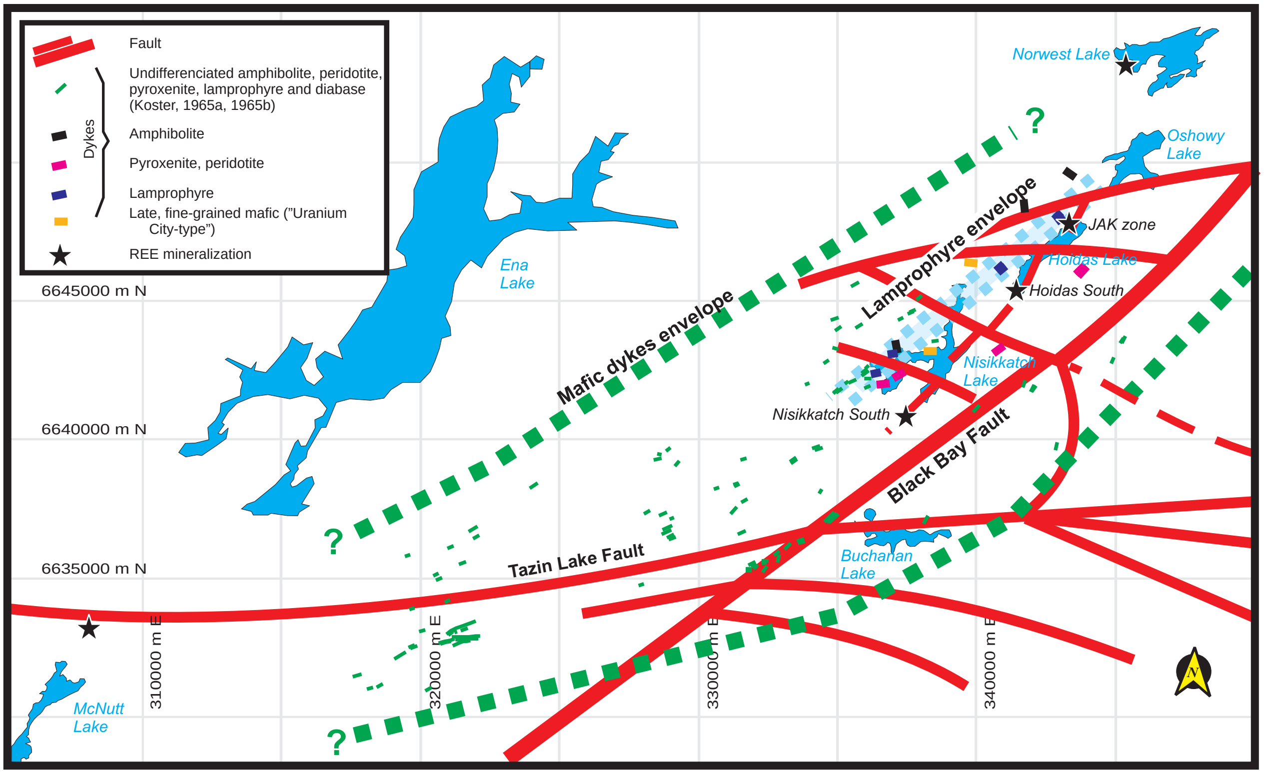

Figure 17 - Map showing the distribution and average orientation of mafic and lamprophyric dykes, and REE mineralization in the northeastern part of the Zemlak domain. The dykes coloured in green were taken from Koster (1965a, 1965b) and consist of a variety of rock types, including amphibolite, peridotite, pyroxenite, lamprophyre, and diabase (they are not differentiated on Koster's maps). The other dykes are from this study. Irrespective of their age and nature, the dykes are concentrated in the Zemlak Domain along a corridor that follows closely the trace of the Black Bay Fault and, in part, the Tazin Lake Fault. The known REE occurrences in the region are located within this corridor. North of Buchanan Lake, the corridor coincides with the highly D_3-strained rocks of the Zemlak Domain, near to and at the contact with the Train Lake Domain. This portion of the corridor, and possibly also the portion located along the Tazin Lake Fault, were active over long periods of time and may define deep-reaching tectonic boundaries. The corridor could be favourable ground for exploration for other syn- to post-D_3 REE mineralization of alkaline affinity.

Our knowledge of the time of emplacement of the REE mineralization in the Hoidas-Nisikkatch lakes area is constrained by a preliminary monazite U-Pb SHRIMP age extracted from one of the mineralized veins (Gunning and Card, 2005). The 1.87 Ga age obtained from this monazite is considerably younger than the 1.911 to 1.903 Ga age for peak metamorphism associated with D_3 in the Uranium City area (Ashton *et al.*, 2009). Taking this 1.87 Ga age as the emplacement age of the REE mineralization, the structural relationships of the mineralized veins suggest that compressive deformation coaxial with D_3 was long lived.

Occurrences of the particular association of calc-silicate–, phosphate- and carbonate-rich mineral assemblages at Hoidas-Nisikkatch lakes are uncommon and poorly understood. Similar zoning patterns and parageneses are reported from veins cutting granulite-facies paragneisses, calc-silicate gneisses, granitic gneisses and granites of Paleoproterozoic age (Bhattacharya *et al.*, 2003) near Kasipatnam, India (Rao, 1976). The Nolans Bore REE-P-U-Th deposit in central Australia also shares a similar geological setting, ore textures and mineralogical assemblages, save for the lack of Ba-rich feldspars (Maas *et al.*, 2009; further information on the Nolans Bore deposit is available at the following link: URL<http://www.ga.gov.au/minerals/research/pubs/presentations/ga2006_16/goulevitch.jsp>).

Although it is widely acknowledged that the REE mineralization at Hoidas Lake has an alkaline affinity, their origin remains to be determined. The mineralized structures contain elevated REE, Th, P, Ba and, to a lesser extent, Sr concentrations, but lack enrichment in Zr/Hf, Nb/Ta, and Ti which are usually associated with carbonatites or agpaitic/peralkaline, silica-saturated or silica-undersaturated systems. In addition, sodic pyriboles are essentially absent (arfvedsonite is reported from the deposit, but is rare and late in the paragenesis), the ferromagnesian minerals being predominantly diopsidic clinopyroxene, hornblende, and biotite. The character of the mineralization shares similarities with carbohydrothermal systems and may represent the distal expression of buried mafic and/or potassic alkaline intrusive rocks. In addition, the deposit may represent an early expression of the alkaline Uranium City mafic dykes and Martin Group mafic volcanic rocks, which would have involved much lower levels of partial melting of the LILE-enriched Rae sublithospheric mantle, consistent with the elevated chondrite-normalized LILE/HFSE ratios of the REE mineralization.

Many questions about such deposits remain: What was the source of the vein material? What was the process that led to vein emplacement? Was a process of liquid immiscibility involved during emplacement of the veins? Further studies are required to assess the relationships between the various facies of the veins. Melt and fluid inclusion, U/Pb, Sm/Nd, Rb/Sr, and C isotopic studies would help clarify the outstanding questions.

7. Acknowledgments

Bill Slimmon and Thomas Love provided assistance in the preparation for field work. Dustin Zmetana prepared the final version of the map that accompanies this report. John Pearson is thanked for providing logistical support and guidance at Hoidas Lake. Colin Card provided valuable information on the geology of the Hoidas-Nisikkatch lakes area. Andrew "Hawkeye" Smith contributed many significant observations during field work. A preliminary version of this report was reviewed by Colin Card and Kate MacLachlan.

8. References

Ashton, K.E. (2009): Compilation Bedrock Geology, Tazin Lake, NTS area 74N; Sask. Ministry of Energy and Resources, Map 246A, 1:250 000-scale map.

Ashton, K.E., Card, C.D., Davis, W., and Heaman, L.M. (2007): New U-Pb zircon age dates from the Tazin Lake map area (NTS 74N); *in* Summary of Investigations 2007, Volume 2, Saskatchewan Geological Survey, Sask. Ministry of Energy and Resources, Misc. Rep. 2007-4.2, CD-ROM, Paper A-11, 8p.

Ashton, K.E., Card, C.D., and Modeland, S. (2005): Geological reconnaissance of the northern Tazin Lake map area (NTS 74N), including parts of the Ena, Nolan, Zemlak, and Taltson domains, Rae Province; *in* Summary of Investigations 2005, Volume 2, Saskatchewan Geological Survey, Sask. Industry Resources, Misc. Rep. 2005-4.2, CD-ROM, Paper A-1, 24p.

Ashton, K.E., Hartlaub, R.P., Heaman, L.M., Morelli, R.M., Card, C.D., Bethune, K., and Hunter, R.C. (2009): Post-Taltson sedimentary and intrusive history of the southern Rae Province along the northern margin of the Athabasca Basin, western Canadian Shield; Precamb. Resear., v175, p16-34.

Ashton, K.E., Kraus, J., Hartlaub, R.P., and Morelli, R. (2000): Uranium City revisited: a new look at the rocks of the Beaverlodge Mining Camp; *in* Summary of Investigations 2000, Volume 2, Saskatchewan Geological Survey, Sask. Energy Mines, Misc. Rep. 99-4.2, p3-15.

Bergeron, J. (2001): The deformational history of the Black Bay structure near Uranium City, northern Saskatchewan; unpubl. M.Sc. thesis, Univ. Saskatchewan, Saskatoon, 250p.

Bergeron, J., Stauffer, M., and Ansdell, K. (2002): The Black Bay deformation zone, Rae Province, Canadian Shield: Archean ductile deformation to Paleoproterozoic brittle slip; 900 my of reactivation; Geol. Assoc. Can./Mineral. Assoc. Can., Jt. Annu. Meet., Saskatoon, Prog. Abstr., v27, p8.

Bhattacharya, S., Kar, R., Teixeira, W., and Basei, M. (2003): High-temperature crustal anatexis in a clockwise P-T-t path: isotopic evidence from a granulite-granitoid suite in the Eastern Ghats belt, India; J. Geol. Soc., London, v160, p39-46.

de Zoysa, T.H. (1974): The Geology of the Ena Lake Area (West Half), Saskatchewan; Sask. Dep. Miner. Resour., Rep. 142, 26p.

Gunning, M.H. and Card, C.D. (2005): Transects across the Black Bay Shear Zone and Hoidas-Nisikkatch Rare-element Trend, northwest Saskatchewan; Sask. Industry Resources, Open File Rep. 2004-2, CD-ROM.

Halpin, K.M., Ansdell, K.M., and Pearson, J. (2008): The Hoidas Lake REE deposit, northern Saskatchewan: a complex apatite-allanite vein system; Geol. Assoc. Can./Mineral. Assoc. Can., Jt. Annu. Meet., Québec, Prog. Abstr., v33, p68.

Harvey, S.E., Young, I., and Billingsley, G. (2002): Geology of the Hoidas Lake area, Ena Domain, northwestern Saskatchewan; *in* Summary of Investigations 2002, Volume 2, Saskatchewan Geological Survey, Sask. Industry Resources, Misc. Rep. 2002-4.2, CD-ROM, Paper C-2, 13p.

Hogarth, D.D. (1957): The apatite bearing veins of Nisikkatch lake, Saskatchewan; Can. Mineral., v6, p140-150.

Koster, R. (1965a): The Geology of the Dardier Lake Area (West Half), Saskatchewan; Sask. Dep. Miner. Resour., Rep. 101, 45p.

__________ (1965b): The Geology of the Ena Lake Area (East Half), Saskatchewan; Sask. Dep. Miner. Resour., Rep. 91, 31p.

Maas, R., Huston, D., and Hussey, K. (2009): Isotopic constraints on the genesis of world-class REE-P-U-Th mineralization, Nolans Bore, Central Australia; Goldschmidt 2009, June 21 to 26, Davos, Switzerland, Abstr., pA809.

Morelli, R.M., Hartlaub, R.P., Ashton, K.E., and Ansdell, K.M. (2009): Evidence for enrichment of subcontinental lithospheric mantle from Paleoproterozoic intracratonic magmas: geochemistry and U-Pb geochronology of Martin Group igneous rocks, western Rae Craton, Canada; Precamb. Resear., v175, p1-15.

Pearson, J.G. (2005): The Hoidas Lake Rare Earth Element Deposit – a progress report; Saskatchewan Geological Survey, Open House 2005, Saskatoon, Nov. 28 to 30, Sask. Industry Resources, Abstr. Vol., p19.

__________ (2006): Geology, setting, and development of the Hoidas Lake Rare Earth Element Deposit; Saskatchewan Geological Survey, Open House 2006, Saskatoon, Nov. 27 to 29, Sask. Industry Resources, Abstr. Vol., p36.

Rao, A.T. (1976): Study of the apatite-magnetite veins near Kasipatnam, Visakhapatnam District, Andhra Pradesh, India; TMPM Tschermaks Min. Petr. Mitt., v23, p87-103.

Thompson, A.B. (1982): Dehydration melting of pelitic rocks and the generation of H_2O-undersaturated granitic liquids; Amer. J. Sci., v282, p1567-1595.

Tremblay, L.P. (1972): Geology of the Beaverlodge Mining Area, Saskatchewan; Geol. Surv. Can., Mem. 367, 265p.

WARDROP (2006): Technical report on the Hoidas Lake Rare Earth Project, Saskatchewan; Project No. 0539480100-REP-L0001-01, 69p.

Winter, J.D. (2001): An Introduction to Igneous and Metamorphic Petrology; Prentice Hall Inc., Upper Saddle River, 697p.

Woolley, A.R. and Kjarsgaard, B.A. (2008): Carbonatite occurrences of the world: map and database; Geol. Surv. Can., Open File 5796, CD-ROM.